

Article

Not peer-reviewed version

The Pyruvate-Glyoxalate Pathway as an Alternative Toxicity Assessment Tool of Xenobiotics: Lessons from Prebiotic Chemistry

[François Gagné](#)* and [Chantale André](#)

Posted Date: 14 November 2025

doi: 10.20944/preprints202509.2418.v2

Keywords: prebiotic chemistry; toxicity; alternative method; fish toxicity; pyruvate; glyoxalate; aldo condensation



Preprints.org is a free multidisciplinary platform providing preprint service that is dedicated to making early versions of research outputs permanently available and citable. Preprints posted at Preprints.org appear in Web of Science, Crossref, Google Scholar, Scilit, Europe PMC.

Copyright: This open access article is published under a Creative Commons CC BY 4.0 license, which permit the free download, distribution, and reuse, provided that the author and preprint are cited in any reuse.

Disclaimer/Publisher's Note: The statements, opinions, and data contained in all publications are solely those of the individual author(s) and contributor(s) and not of MDPI and/or the editor(s). MDPI and/or the editor(s) disclaim responsibility for any injury to people or property resulting from any ideas, methods, instructions, or products referred to in the content.

Article

The Pyruvate-Glyoxalate Pathway as an Alternative Toxicity Assessment Tool of Xenobiotics: Lessons from Prebiotic Chemistry

Gagné F. * and André C.

Aquatic Contaminants Research division, Environment and Climate Change Canada, Montréal, QC, Canada

* Correspondence: francois.gagne@ec.gc.ca

Abstract

There is an urgent need to evaluate the toxicity of xenobiotics and complex mixtures the prevention the degradation of water quality sustaining aquatic ecosystems. A simple biogenic chemical pathway based on malate formation from pyruvate (pyr) and glyoxalate (glyox) pathway is proposed as quick and cheap screening tool for toxicity assessment. The assay is based on pyr and glyox (aldol) pathway leading to biologically relevant precursors such as oxaloacetate and malate. Incubation of pyr and glyox at 40-70°C in the presence of reduced iron-Fe(II) led to malate formation following the first 3 h of incubation. The addition of various xenobiotics/contaminants (silver, copper, zinc, cerium IV, samarium III, dibutylphthalate, 1,3-diphenylguanidine, carbon-walled nanotube, nanoFe₂O₃ and polystyrene nanoparticles) led to inhibitions in malate synthesis at various degrees. Based on the concentration inhibiting malate concentrations by 20% (IC₂₀), the following potencies were observed: silver < copper ~1,3-diphenylguanidine ~ carbon walled nanotube < zinc ~ samarium < dibutylphthalate ~ samarium < Ce(IV) < nFeO₃ < polystyrene nanoplastics. The IC₂₀ values were also significantly correlated with the reported trout acute lethality data suggesting its potential use as screening toxicity test. The pyr-glyox pathway was also tested on surface water extracts (C18) and identified the most contaminated sites from large cities and municipal wastewater effluents. The inhibition potencies of the selected test compounds revealed that not only pro-oxidants are associated to toxicity but chemicals hindering enolate formation, nucleophilic attack of carbonyls and dehydration involved in aldol condensation reactions were also associated to toxicity. The pyr-glyox pathway is based on a fundamental aspect of chemical reactions during the emergence of life and represents a unique tool to identify toxic compounds individually and in complex mixtures.

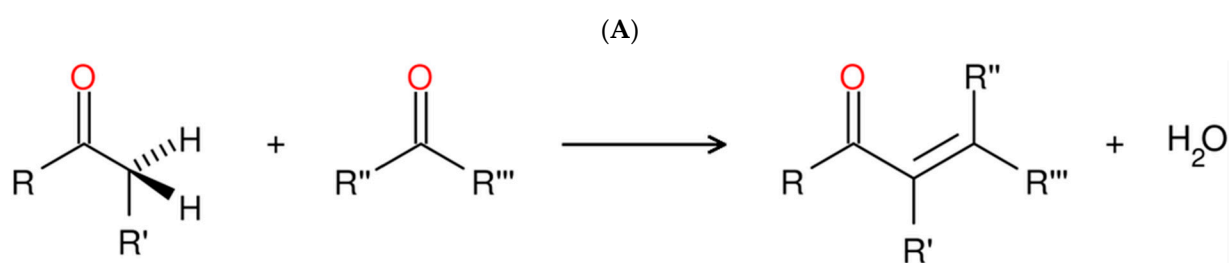
Keywords: prebiotic chemistry; pyruvate-glyoxalate pathway; biotest; fish alternative

1. Introduction

Aquatic ecosystems are subjected to multiple sources of pollution releasing thousands of human-made xenobiotics through water (wastewaters and rainfall runoffs), air (dust, volatile compounds) and solids (solid waste, electronic waste, etc). It is generally accepted by the scientific community that relying only on the physico-chemical properties of water is incomplete and requires toxicity assessments, which integrates the whole mixture effects and unknown chemicals [1]. The ongoing toxicity evaluation of these complex mixtures is nowadays an integral part of ecotoxicological risk assessment strategies. In the context of environmental protection strategies and law enforcement, bioassays investigating the toxicological properties of these chemicals and mixtures represent an ongoing effort for ensuring sustainability of our economy. Bioassays usually encompass the selection of sentinel species at specific levels of the food chain where fish toxicity information is mandatory since it is protected and recognized by law [2]. For example, a test battery encompassing bacteria, algae/plants, invertebrates (worm, crustacean and bivalve) and vertebrates (fish and amphibians) helps identify the most sensitive species [3] and elaborate a toxicity distribution often used for

probabilistic risk assessments of chemicals of emerging interests [4]. Fish toxicity testing for regulatory purposes leads to the sacrifice of tens of thousands of fish per country. In this context, alternative methods to limit fish use are welcome for ethical and practical consideration. Different types of alternatives exist albeit not systematically validated: fish at the hatching/larval stage, alternate organism (usually an invertebrate), in vitro (cells) methods, biosensors (enzymes), biochemical pathways and artificial intelligence modelling in identifying potentially toxic chemicals based on various chemical properties. For example, the *Hydra vulgaris* bioassay and the peroxidase biosensor hold promise as alternatives given their high sensitivity and predictability towards rainbow trout acute lethality test for law enforcement [5,6]. Metabolic pathways have yet to be considered as alternative tests although their potential to deliver cost-effective biotests. Metabolic pathways essentially determine whether xenobiotics could dampen parts of crucial metabolic networks such as the tricarboxylic acid (TCA) cycle for energy metabolism and cellular respiration involving the 5 universal intermediates: acetate, pyruvate, oxaloacetate, succinate and α -ketoglutarate found in all life forms [7].

In the selection of metabolic pathways as potential targets, primitive metabolic pathways thought to originate in early Earth before the formation of organized cells could be ideal candidates. These pathways intervene during the first prebiotic chemical reactions during the Hadean era of Earth [8]. These protometabolic networks could serve as toxicity alternatives provided that the generated toxicity data predicts toxicity. The TCA cycle has been an attractive target given that virtually all anabolic pathways in the metabolic pathways chart originate from the TCA cycle ([metabolic pathways chart](#)) [9]. Genomic studies suggest that an ancestor of the TCA cycle was formed in the making of intermediates such as sugars, amino acids and lipids. So-called the reverse TCA (rTCA), it was autocatalytic before the formation of enzymes provided the intermediates were maintained in the cycle leading to the mobilization of carbon from the reduction of CO₂ (abundant during early earth). Indeed, the capacity of iron to promote the rTCA variant from simple prebiotic precursors - pyruvate (pyr) and glyoxalate (glyox) was experimentally established [10]. In addition, pyr and glyox could be produced from abiotic processes of atmospheric CO₂ fixation by reduced iron [11]. Reduced iron Fe(II) was/is one of the most abundant metals in Earth's crust and large amounts of Fe(II) prior to the rise of oxygen was readily available [12]. The reaction is surprisingly simple requiring only heating a mixture of pyr, glyox and Fe(II) under inert conditions (N₂ atmosphere) for a few hours. This led to the formation of highly interconnected pathways capable of both anabolic and catabolic activities involving 5 main reaction mechanisms: decarboxylation, reduction/oxidation, dehydration/hydration, and aldol/retro-aldol reactions. Aldol condensation, in turn, involves the formation of enolate ions (pyr), nucleophilic attack on the carbonyl/aldehyde carbon and dehydration (Figure 1). It is theorized that xenobiotics hindering these prebiotic reactions have the potential to initiate toxicity.



Aldol condensation: enolate formation (R-CO-R'), nucleophilic attack at the carbonyl and dehydration leading to double bond formation.

(B)

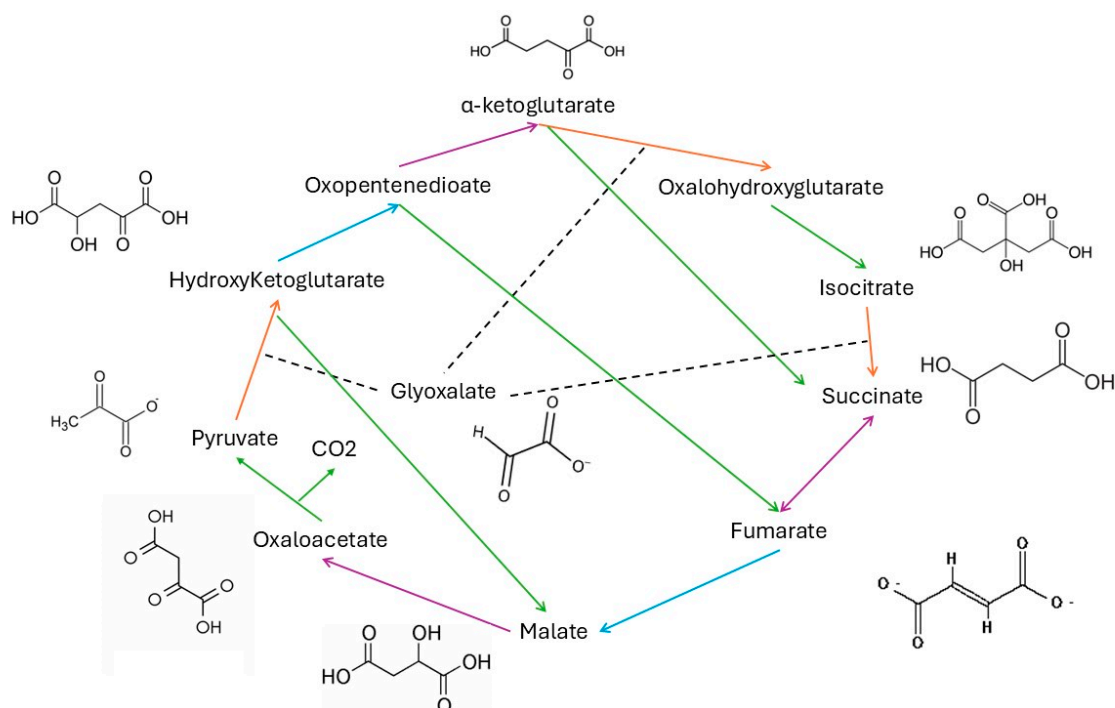


Figure 1. The pyruvate glyoxalate pathway. The pyr-glyox pathway starts with aldol reaction depicted in A. The pathway between pyruvate and glyoxalate in the presence of reduced Fe^{2+} (B). The cycle involves aldol/retroaldol condensation (orange lines, e.g. pyr + glyox \rightarrow hydroxyglutarate and isocitrate \rightarrow succinate + glyoxalate for aldol and retroaldol reactions respectively), hydration/retrohydration (blue line, e.g. hydroxyglutarate \rightarrow oxopentenedioate), oxidative decarboxylation (green arrows oxalohydroxyglutarate \rightarrow isocitrate + CO_2), reduction/oxidation (violet arrows, e.g. succinate \rightarrow fumarate). From [9].

The purpose of this study was therefore to examine the pyr-glyox pathway to probe the effects of selected xenobiotics and mixtures (surface wastewaters extracts) in the formation of the end product malate. The hypothesis states that xenobiotics capable of hindering malate formation from the primitive pyr-glyox pathway are related to toxicity. The influence of 10 well known contaminants of emerging interests (plasticizers, endocrine disruptors, plastic/carbon/iron-based nanoparticles, tire wear substances, metals and rare earth elements) toward the inhibition of the pyr-glyox pathway was examined and compared to fish mortality data. Moreover, malate production was examined in real-life river water and wastewater extracts (mixtures) to determine the most impacted/polluted samples. An attempt was made to understand the role of ancient metabolic pathways towards initiation of toxicity beyond the oxidative stress paradigm during the initiation of toxicity [13].

2. Materials and Methods

2.1. Chemicals and Water Extraction

The following chemicals were purchased at 99% purity for copper (CuCl_2), silver (AgNO_3), samarium (SmCl_3), cerium (CeCl_4), zinc (ZnSO_4), the plasticizer/endocrine disruptor dibutylphthalate (DBP) and tire related compound 1,3-diphenylguanidine (1,3-DPG) were purchased from Sigma Chemical Company (On, Canada). They were prepared in MilliQ water at 1mg/mL with the exception DBP and 1,3-DPG which were prepared in ethanol at the same concentration. Polystyrene nanoparticles of 20 nm diameter were purchased from ThermoFischer Scientific (USA). It was diluted in MilliQ water at 0.1 %. Carbon nanotubes (CNT) of 5-10 nm internal diameter/1-3 μm fiber length and iron (II) nanoparticles ($\text{nFe(II)}_2\text{O}_3$, 30 nm diameter) were purchased at US Research Nanomaterials (Houston, TX, USA). They were diluted at 10 mg/mL in MilliQ water to prevent

aggregation [14]. The stock solutions were prepared the day before the exposure experiments. All concentrations are nominal concentrations.

Surface waters, untreated wastewaters (influent) and treated wastewaters (effluent) were collected as composites of surface waters (3 x 1l samples per sites) and 24h composites (1 l) for surface waters and municipal wastewaters respectively. The surface water were collected in the Saint-Lawrence in the Montreal area: at the mouth of the Chateaugay river (CHA) on the south shore of the island of Montreal, one site 8 km downstream the City of Montréal (Downs), at the marina of the city of Lavaltrie (LA) located some 40 km downstream of the island of Montreal on the north shore of the Saint-Lawrence river. The untreated (influent) and treated wastewaters (effluent) were collected from typical city with a population of circa 100 000 residents using a primary clarifier (ferric chloride to remove phosphates) followed by an activated sludge and chlorine disinfection (sodium sulfite for dichlorination) treatments. A volume of 200 mL sample was filtered on 0.8 µm cellulose acetate membrane for the removal suspended solids and the filtrate passed through a C18 solid phase extraction cartridge (Bond Elut, 100 mg bed mass), washed with 5 mL of MilliQ water and eluted with 0.5 mL ethanol corresponding to 400 X concentrates. The ethanol extracts were kept at 4°C until analysis the same week.

2.2. Pyruvate-Glyoxylate Assay

The pyruvate-glyoxylate assay was prepared following a modification of a previously reported methodology [9,10]. The main modifications were the reduction of reactant concentrations to increase its sensitivity to exposure to various chemicals and complex mixtures in the environment and the optimal detection of the end products malate and oxaloacetate using an enzyme detection system. Briefly, 1 mM of sodium pyruvate, 2 mM glyoxalate and 4 mM FeSO₄ were prepared in 1 mL of MilliQ water at pH 6.5 with increasing concentrations (in separate tubes: control, 4, 20 and 100 mg/L) for each of the 10 contaminants highlighted above or water extracts (in separate tubes: control, 0.8, 4 and 20X). The assay tube were prepared in duplicate samples and the experiment repeated 3 times. The mixture was degassed under N₂ stream and incubated at 70°C for 3h. The controls contained only MilliQ water or the equivalent amount of ethanol (C18 extract solvent; final concentration of 5% for the 20X concentration). The reaction was cooled down at room temperature and the levels of malate were determined by malate dehydrogenase enzyme system. The reaction tubes appeared yellow dark from Fe(II) and no observation of turbidity. A 10-20 µl sample of the reaction mixture was mixed with 1 mM NAD⁺ in the assay buffer composed of 140 mM NaCl, 1 mM MgCl₂ and 20 mM Tris base, pH 8.5 in 96-well dark microplates. The reaction was initiated by adding 10 µL of 10 units of malate dehydrogenase (10 units of MDH; Sigma Chemical Company, On, Canada). An operational blank was composed of NAD⁺ alone. Malate standards (0.05-0.15 mM) in the presence of NAD⁺ and MDH were also included for calibration. The formation of reduced NADH was measured for 20 min at 1 min intervals by fluorescence at 350 nm excitation and 450 nm emission wavelengths using a microplate reader (Synergy IV, Biotek instruments, CA, USA). The rate of NADH formation was calculated for 10 min and used to determine the formation of malate in duplicate assay samples The data was expressed as relative fluorescent unit (RFU)/min.

2.3. Rainbow Trout Acute Lethality Tests

The rainbow trout (*Oncorhynchus mykiss*) or other fish species (*Channa punctatus*, *Oryzias latipe* and *Cyprinus carpio*) acute toxicity data were provided in the literature for the tested compounds (with the exception of PSNPs) for comparison of malate inhibition with toxic effects on trout survival. With the exception of PSNPs and 1,3-DPG, the acute lethality tests were performed following the standard protocol of Environment and Climate Change Canada [15]: Biological test method: acute lethality test using rainbow trout - Canada.ca. Briefly, 10 newly hatched juveniles with the egg yolk sac fully reabsorbed (0.3–2.5 g) were placed in 60 L containers lined with polyethylene bags and exposed to increasing concentrations of PsNPs (100, 50, 10, 2 and 0.4 mg/L) for 96 h at 15 °C under constant aeration. The fish were not fed during the exposure period and distressed fish were

examined twice daily and immediately euthanized in 50 mg/L tricaine sulphate as per the animal care committee recommendations. A positive control (ZnSO₄; LC₅₀ 0.4 mg/L (0.09-1 95% interval confidence) was also used to ensure reproducibility of the fish toxicity test.

2.4. Data Analysis

The experiments were repeated N=3 times and the data were subjected to an analysis of variance after checking for data homogeneity using Levene's and Shapiro-Wilk's tests. In the case of non-parametric data, the data were log transformed. Critical differences between controls and exposure concentrations were determined by the Least Square Difference test. The calculation of the concentration of the test samples that inhibited malate formation by 20% (IC₂₀) was calculated based on graphical extrapolation of the concentration-response responses curves. The lethal concentration that caused trout mortality by 50% (LC₅₀) was calculated by the Spearman-Kärber methodology [16]. The data were expressed in mg/L for single substances and X fold concentration for complex mixtures (C18 ethanol extracts) where 1 X concentration corresponds to the original undiluted water sample.

3. Results and Discussion

The pyr-glyox reaction involves a series of aldol condensation, redox and dehydration reactions as depicted in Figure 1A. The newly formed metabolite hydroxyglutarate from glyox and pyr undergoes a series of hydration/dehydration, oxydo/reductive and additional aldol condensation reactions forming more complex molecules such as citrate, succinate, malate and oxaloacetate (Figure 1B). The source of electrons is assured by Fe(II), which represents one of the most abundant and available metal in Earth crust prior to the Grand Oxidation event [12]. When glyox and pyr are added at a molar ration 2:1 in the presence of 4 equivalents of reduced Fe(II) in MilliQ water, malate (and oxaloacetate) was detected following 1 to 3 hr incubation at 70°C (Figure 2). Longer exposure times to 24h lead to increased levels of malate as well using the original protocol but malate levels did not increase after 4 h when using lower concentrations of pyr, glyox and Fe(II). Indeed, the initial protocols used concentration in the 0.1 to 0.4 M range, representing concentration levels much higher than environmental contaminants. The concentration was downscaled to the mM range, which improved the sensitivity of the assay towards environmental pollutants permitting malate detection using malate dehydrogenase assay. In these conditions, longer exposure times (24 h) at 70°C did not lead to significant increase in malate, probably by saturation of the reaction or heat degradation. Hence, for toxicity experiments the following concentrations of the reagents were used: 1 mM Pyr, 2 mM glyoxalate and 4 mM Fe(II) at 70°C for 3h.

The pyr-glyox pathway was examined with increasing concentrations of the selected environmental contaminants (Figure 3A). The figure shows that increasing the concentrations of Ag, Zn and 1,3-DPG decreased production of malate at various degrees of intensity. Not only the pro-oxidants compounds Ag⁺ decreased malate production but zinc and 1,3-DPG (a tire related compound) as well. This tire wear compound (1,3-DPG) was less potent to the inhibition of malate production. This suggests that not only oxidants can inhibit the pyr-glyox pathway but other chemicals (reductants) as well. It is generally thought that the oxidative properties compounds are one of the main drivers of toxicity of xenobiotics [13]. The concentration that inhibits malate concentration by 20% (IC) was calculated and reported in Table 1. The IC₂₀ spans from 1 to 150 mg/L with the following decreasing potency to inhibit the pyr-glyox reaction: Ag > Cu ~1,3-DPG ~ carbon walled nanotube > Zn > DBP > Sm > Ce(IV) > nFeO₃ > polystyrene nanoplastics. In respect to fish toxicity, the LC₅₀ ranged from 0.1 to 100 mg/L in the following decreasing order of toxicity: Ag > Cu > Zn ~ Sm ~ DBP > 1,3-DPG > carbon walled nanotubes > nFe₂O₃ > polystyrene nanoplastics. Based on these distributions, it appears that the pyr-glyox pathway is as sensitive to oxidants than fish based on copper and Ag responses albeit at concentrations 10 times higher than for rainbow trout. This could be attributed to the initial concentration of pyr (87 mg/L) and glyox (140 mg/L) used here but could be reduced at lower concentrations permitted by the malate detection system in place. The pyr-glyox reaction seems to respond more to electron donors (reductants) than rainbow trout such as 1,3-

DPG and carbon (graphene) walled nanotubes in the presence of reduced iron Fe(II). Aldol condensation involves 3 major steps the formation of the enolate ion where the mobility of hydrogen at the α carbon (of an $C^{\alpha}-H^{\beta}$) next to carbonyl (pyruvate) could be inhibited by xenobiotics such as guanidines or acidic groups (carboxylic acid, thiols) in alkaline conditions [17]. Hence, this encompasses a large range of polar compounds such as pesticides, pharmaceuticals and industrial pollutants. For example, guanidines are used in the production of plastics (plastic tubing in households) and tire rubbers such as 1,3-DPG and 2-cyanoguanidine [18]. They are also considered chaotropic agents able to denature proteins and nucleic acids [19,20]. The former study also showed that excess oxidized Fe(II), cadmium, lead, manganese and aluminum were also able to inhibit this reaction perhaps at the second step involving the nucleophilic reaction of the enolate ion. The guanidine containing drug metformin was shown to inhibit aconitase reaction involving the dehydration of isocitrate to citrate in the tricarboxylic acid cycle suggesting interactions at the 3rd step of aldol condensation as well [21]. Acrylamide and nucleophile maleimide were also shown to disrupt the cyclic production of thiol from amino acids thioester conjugates, which also involve nucleophilic reactions with thiols as with aldol reactions [22]. This suggests that electron donors/nucleophiles (RSH, maleimides, amines etc) could inhibit the pyr-glyox pathway but at different steps of the aldol condensation reactions. The aldol condensation of 2-keto-4-hydroxybutyrate from glyox and pyr catalyzed by aldolase in bovine liver and *Escherichia coli* also revealed inhibitions by various agents [23]. It was found that halides (anions) and carboxylic acids were inhibitors while esters were not as potent inhibitors of the condensation reaction of glyox and pyr. Mono-, di-, and tricarboxylic acids were proportionally inhibitory and hydroxypyruvate (blocks the mobility of H^+ at the α carbon and the formation of enolate ion) was the most potent inhibitor. Increasing the concentration of glyox relative to pyr was also inhibitory perhaps through the enzyme inactivation by this aldehyde. Hence, the pyr-glyox reaction involves reactions beyond the classic oxidative paradigm of toxic compounds. Indeed, compounds able to disrupt the formation of enols from the mobility of hydrogen of α carbon adjacent to carbonyl, block/competitive nucleophilic reaction to aldehydes and dehydration steps are involved in the pyr-glyox pathway where inhibitions in these reactions could initiate toxicity at the molecular level.

Table 1. Selected compounds for the pyr-glyox reactions.

Compounds	Pyr-Glyox (IC20 mg/l)	Trout toxicity (LC50 mg/l)	References
Dibutylphthalate (DBP)	35	1.6	[31]
1,3-Diphenylguanidine (1.3-DPG)	12	4.2	Registration Dossier - ECHA
Copper Cu(II)	12	0.1	[32]
Silver Ag(I)	1	0.02	[32]
Zinc Zn(II)	41	1.6	[32,33]
Samarium Sm(III)	24	2	[34]
Cerium Ce(IV)	77	95	[34]
nFe_2O_3	146	100 (<i>Oryzias latipes</i> embryo)	[35]
Polystyrene nanoplastic (PSNP)	150	>100	This lab (section 2.3)
Carbon walled nanotubes (CNT)	17	22 (<i>Channa punctatus</i> juvenile)	[25]

In the attempt to provide a toxicological meaning towards this prebiotic reaction network, the malate IC20 was compared with the rainbow trout acute lethality tests (Figure 3B). The data show that concentrations able to reduce malate production was significantly correlated to trout toxicity

(LC50) data ($r=0.84$; $p<0.001$). The LC50 value of PSNP was set at 100 mg/L ($\log\text{LC50}=2$) since it was reported that this plastic induces oxidative stress and damage at these concentrations [26]. This suggests that compounds able to inhibit aldol-condensation and/or redox properties are involved in the toxicity of these substances. These reactions take place in the TCA cycles present today where inhibitions in these reactions will decrease energy production and cellular respiration rates. This could form the basis of toxicity initiation in organisms. The oxidative properties of xenobiotics represent one of the most fundamental interactions in toxicity initiation [13,24]. From the 10 selected compounds, 3 were nanoparticles (nFe₂O₃, PSNPs and CNT) and were shown to reduced malate production at relatively higher concentrations (20-100 mg/L), in keeping with their relatively low toxicity (compared to Ag or Cu) in fish and hydra in previous studies [25,26]. However, plastic nanoparticles and CNT produce oxidative stress at the mg/L range in hydra [27,28] suggesting impacts at longer exposure times. In this respect, the pyr-glyox pathway could serve as generic test for toxicity screening of miscellaneous chemicals and mixtures. Keeping this in mind, we used the pyr-glyox reaction on C18 ethanolic extracts of various surface waters and municipal effluents (Figure 4). The samples consisted of various environmental liquids such as river water (CHA, LA, Downs), untreated (influent) and treated effluents. The data revealed that river water samples did not produce significant changes in the reaction at concentration reaching 20X of the water sample. The downstream site (DOWNS, 10 km downstream) of a 1.8 million population city inhibited the pyr-glyox pathway at 20 X concentration and to some extent at 4X but not at environmentally realistic concentration since no significant changes occurred at < 1 X (0.8) concentration. While the influent did not produce any significant changes in malate levels, the treated municipal effluent however, significantly inhibited malate formation at concentrations of 0.8 X and higher. This suggests that this effluent might pose a risk to aquatic life near the discharge point. In order to preserve anonymity of the city involved, fish toxicity of this effluent was previously reported on some occasions. This effluent is produced from an activated sludge effluent with residency times of 10-20 days where ferric chloride for phosphate removal and disinfection (UV) steps was applied. Activated sludges of a city of similar size revealed substantial amounts of plastic (polystyrene) polymers (10-20 $\mu\text{g/L}$) and polyaromatic hydrocarbons (30-40 $\mu\text{g/L}$) in effluents [29]. The levels of melamine and polystyrene nanoplastics in the effluents were higher than in the influent, suggesting that sustained effluent treatment breaks down the suspended organic matter leading to the release of dissolved components such as melamine-based products (paints and panels) and plastic nanoparticles [30]. This could explain why stronger inhibitions were observed in this secondary treated aeration sludge effluents than the other samples. Moreover, 1,3-DPG (0.04 $\mu\text{g/L}$) and cyanoguanidine (2.4 $\mu\text{g/L}$), constituents of tire and tire wear dusts, are finding their way in the dissolved fraction of municipal effluents [31].

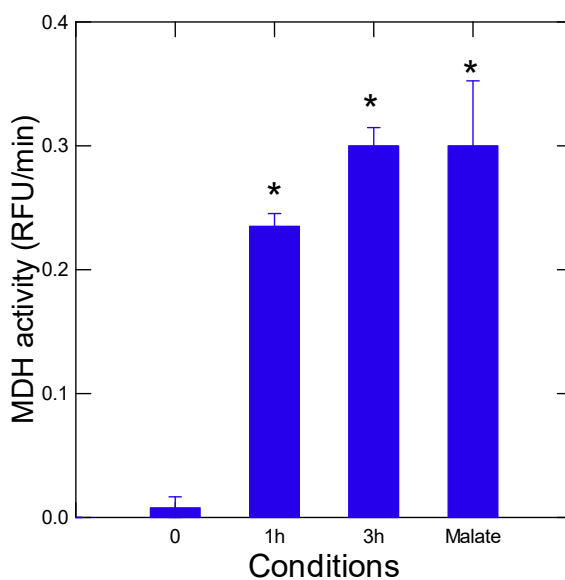


Figure 2. Formation of malate following incubation of pyruvate and glyoxalate. Pyr, glyox and reduced iron (Fe^{2+}) were allowed to react at 70°C for 1 and 3 h. Malate levels were determined by the NAD^+ malate dehydrogenase system. A gradual increase in malate is observed relative to initial time 0h at 1 and 3h incubation time. The last column represents a malate standard ($0.5 \mu\text{M}$) added as a positive control for the malate detection kit. The star symbol indicates significance at $p < 0.05$.

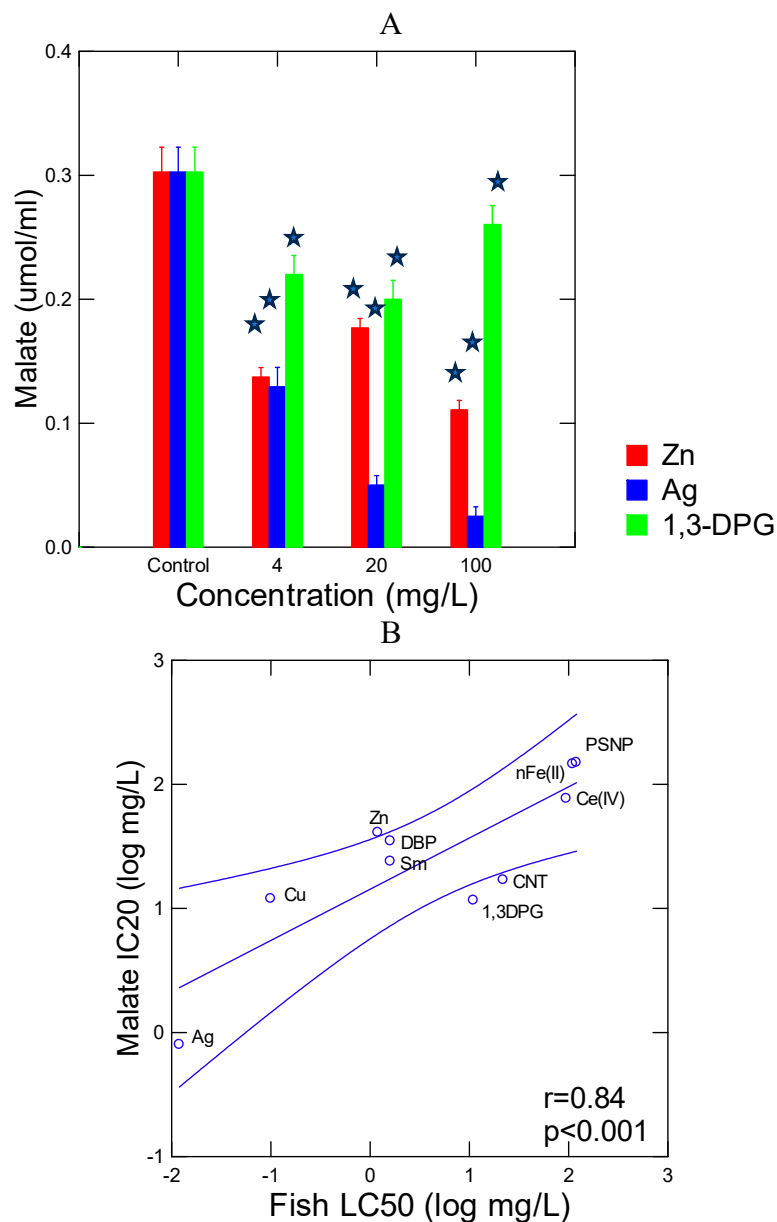


Figure 3. Representation responses of malate formation inhibitions by selected toxic compounds towards rainbow trout. Representative inhibition profiles of malate production (A) and regression analysis of malate inhibition ($\log \text{IC}_{20} \text{ mg/l}$) and 96h trout mortality ($\log \text{LC}_{50} \text{ mg/l}$) (B) from reported literature data. The regression slope between the IC_{20} of the pyr-glyox reaction and trout 96h LC_{50} was obtained from $N=10$ compounds reported in table 1: DBP, 1,3-DPG, Cu, Ag, Zn, Sm, Ce(IV), PSNPs, CWNT and $\text{nFe(II)}_3\text{O}_4$.

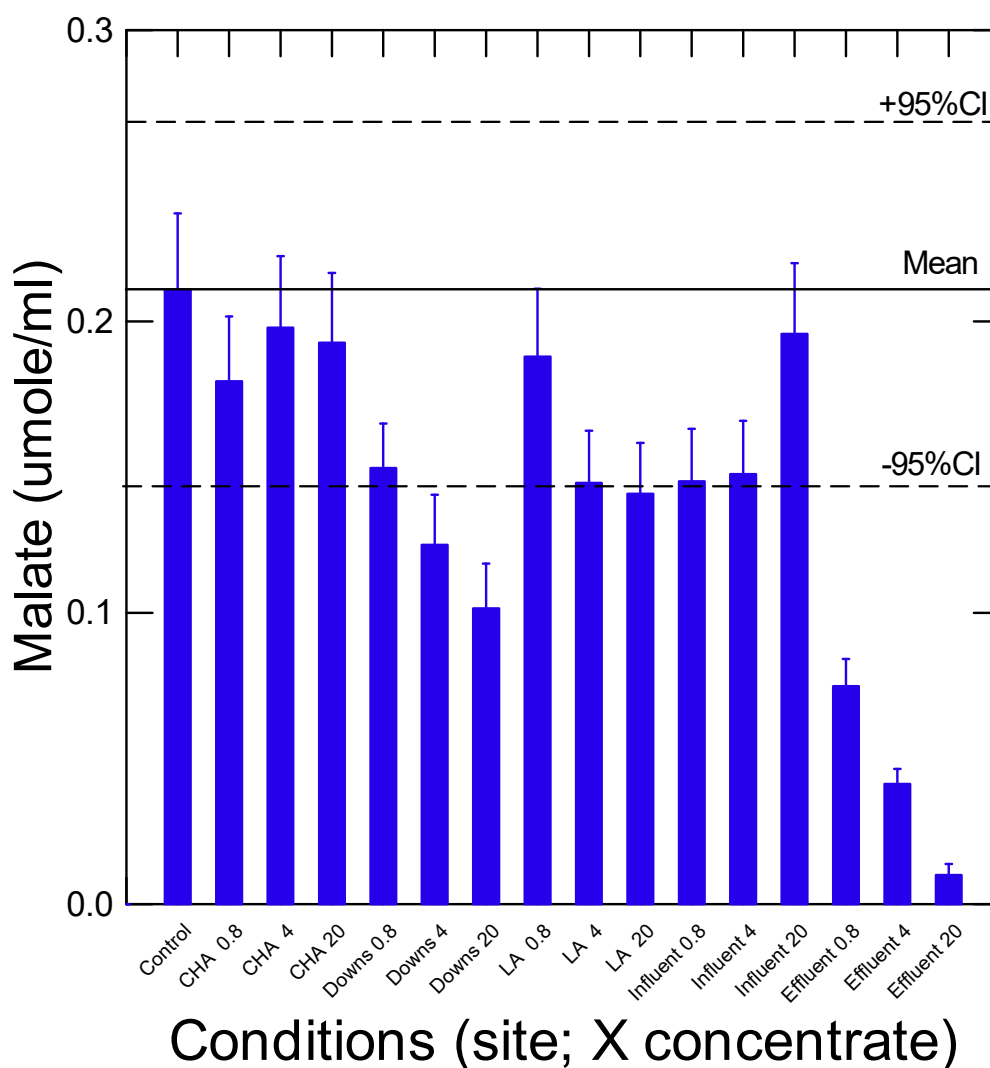


Figure 4. Influence of surface and wastewaters to the pyr-glyox pathway. Surface water and municipal influent/effluent extracts were examined with the pyr-glyox assay in triplicates (N=3). The identification of the tested water samples and exposure concentration (expressed as X fold concentration) are identified on the abscissa axe.

In conclusion, a rapid and cost-effective chemical test is proposed as a screening tool for miscellaneous environmental liquids. The chemical is based on biochemical reactions between biogenic precursors pyr and glyox as primitive biochemical pathways thought to originate in early earth. The inhibition potencies of the selected test compounds revealed that not only pro-oxidants are associated to toxicity but chemicals hindering enolate formation, nucleophilic attack of carbonyls and dehydration. Furthermore, comparative analysis with fish toxicity (LC50) of pyr-glyox inhibitions revealed a significant correspondence for the 10 compounds tested here making this test a useful screening test to identify potential toxic compounds. However, future research is necessary to validate this relationship and should be further investigated with other toxic xenobiotics.

References

1. Ten Brink, B.J.E., Woudstra, J.H. Towards an effective and rational water management: the aquatic outlook project-integrating water management, monitoring and research. *Eur. Water Pollut. Control* 1991, 1, 20–27.
2. Fishery Act. Published by the Minister of Justice 2025, R.S., c. F-14, s. 1, Canada, 111p.

3. Costan, G., Bermingham, N., Blaise, C., Ferard, J.F. Potential ecotoxic effects probe (PEEP): a novel index to assess and compare the toxic potential of industrial effluents. *Environ. Toxicol. Wat. Qual.* 1993, 18, 117–140.
4. Yang, H., Sun, F., Liao, H., Guo, Y., Wang, J., Wu, F. Quantitative characteristics and multiple probabilistic risk assessment of small-sized microplastics in the middle and lower reaches of the Hanjiang River, China. *Mar. Poll. Bull.* 2025, 220, 118404.
5. Farley, G., Bouchard, P., Faille, C., Trottier, S., Gagné, F. Towards the standardization of *Hydra vulgaris* bioassay for toxicity assessments of liquid samples. *Ecotoxicol. Environ. Saf.* 2025, 290, 117560.
6. Gagné F., Roubeau Dumont, E., Chantale, A. The effects of selected metals and rare earth elements on the peroxidase toxicity assay. *Adv. Earth Environ. Sci.* 2025, 6, 1-8.
7. Braakman, R., Smith, E. The compositional and evolutionary logic of metabolism. *Phys. Biol.* 2013, 10, 011001.
8. Nogal, N., Sanz-Sanchez, M., Vela-Gallego, S., Ruiz-Mirazo, K., de la Escosura, A. The protometabolic nature of prebiotic chemistry. *Chem. Soc. Rev.* 2023, 52, 7359.
9. Tran, P.Q., Adam, Z.R., Fahrenbach, A.C. Prebiotic Reaction Networks in Water. *Life* 2020, 10, 352, doi:10.3390/life10120352.
10. Muchowska, K.B., Varma, S.J., Moran, J. Synthesis and breakdown of universal metabolic precursors promoted by Iron. *Nature* 2019, 569, 104–107.
11. Varma, S.J., Muchowska, K.B., Chatelain, P., Moran, J. Native iron reduces CO₂ to intermediates and end-Products of the acetyl-CoA Pathway. *Nat. Ecol. Evol.* 2018, 2, 1019–1024.
12. Emsley, J. *The Elements* 2019, Oxford University Press, NY, USA, 256 pp.
13. Villamena, F., Forman, H.J. *Molecular basis of oxidative stress: chemistry, toxicology, disease pathogenesis, diagnosis, and therapeutics*, John Wiley & Sons, Inc. January 2025 ISBN:9781119790266.
14. Shrestha, S., Wang, B., Dutta, P. Nanoparticle processing: Understanding and controlling aggregation. *Adv. Coll. Interf. Sci.* 2020, 279, 102162.
15. Environment Canada. Biological test method: acute lethality test using rainbow trout environmental protection series 2007, report EPS 1/RM/9.
16. Finney, D.J. *Statistical Method in Biological Assay*; Hafner Publishing Company: New York, NY, USA, 1964, 668p.
17. Bhajiwala, H.M., Patil, H.R., Gupta, V. Studies of amino acids for inhibition of aldol condensation and dissolution of polymeric product of aldehyde in alkaline media. *Appl. Petrochem. Res.* 2013, 3, 17–23. <https://doi.org/10.1007/s13203-013-0025-y>.
18. dos Santos, M.M., Snyder, S.A. Occurrence of polymer additives 1,3-Diphenylguanidine (DPG), *N*-(1,3-Dimethylbutyl)-*N'*-phenyl-1,4-benzenediamine (6PPD), and chlorinated byproducts in drinking water: contribution from plumbing polymer materials. *Environ. Sci. Technol. Lett.* 2023, 10, 10, 885–890.
19. Maxwell, K.L., Bona, D., Liu, C., Arrowsmith, C.H., Edwards, A.M. Refolding out of guanidine hydrochloride is an effective approach for high-throughput structural studies of small proteins. *Protein Sci.* 2003, 12, 2073-80. doi: 10.1110/ps.0393503.
20. Blanco, F., Kelly, B., Sánchez-Sanz, G., Trujillo, C., Alkorta, I., Elguero, J., Rozas, I. Non-covalent interactions: complexes of guanidinium with DNA and RNA nucleobases. *J. Phys. Chem. B* 2013, 117, 11608-16. doi: 10.1021/jp407339v.
21. Gasmi, A., Peana, M., Arshad, M., Butnariu, M., Menzel, A., Bjørklund, G. Krebs cycle: activators, inhibitors and their roles in the modulation of carcinogenesis *Arch. Toxicol.* 2021, 95, 1161–1178.
22. Cafferty, B.J., Wong, A.S.Y., Semenov, S.N., Belding, L., Gmür, S., Huck, W.T.S., Whitesides, G.M. Robustness, entrainment, and hybridization in dissipative molecular networks, and the origin of life. *J. Am. Chem. Soc.* 2019, 141, 8289–8295.
23. Grady, S.R., Wang, J.K., Dekker, E.E. Steady-state kinetics and inhibition studies of the aldol condensation reaction catalyzed by bovine liver and *Escherichia coli* 2-keto-4-hydroxyglutarate aldolase. *Biochemistry* 1981, 20, 2497-2502.
24. Deavall, D.G., Martin, E.A., Horner, J.M., Roberts, R. Drug-Induced Oxidative Stress and Toxicity. *J. Toxicol.* 2012, 645460. doi: 10.1155/2012/645460

25. Ali, D., Falodah, F.A., Almutairi, B., Alkahtani, S., Alarifi, S. 2020. Assessment of DNA damage and oxidative stress in juvenile *Channa punctatus* (Bloch) after exposure to multi-walled carbon nanotubes. *Environ. Toxicol.* 2020, 35, 359-367, 10.1002/tox.22871.
26. Guo Z, Yang R, Hua Z, Long W, Xiang Q. Effect of polystyrene nanoplastics on the intestinal histopathology, oxidative stress, and microbiota of *Acrossocheilus yunnanensis*. *Aquat Toxicol.* 2025, 283:107359.
27. Auclair, J., Quinn, B., Peyrot, C., Wilkinson, K.J., Gagné, F. Detection, biophysical effects, and toxicity of polystyrene nanoparticles to the cnidarian *Hydra attenuata*. *Environ. Sci. Poll. Res. Int.* 2020, 27, 11772-11781.
28. Auclair, J., Roubeau Dumont, E., Gagné, F. Lethal and sublethal toxicity of nanosilver and carbon nanotube composites to *Hydra vulgaris*—A toxicogenomic approach. *Nanomaterials* 2024, 14, 1955. DOI: <https://doi.org/10.3390/nano14231955>.
29. André, C., Smyth, S.A., Gagné, F. The peroxidase toxicity assay for the rapid evaluation of municipal effluent quality. *Water Emerg. Contam. Nanoplast.* 2025, 101, 2.
30. Gagné F., André C., Smyth S.-A. Screening of municipal effluents with the peroxidase toxicity assay. *Disc. Wat.* 2024, 4, 101.
31. Ichihara, M., Asakawa, D., Yamamoto, A., Sudo, M. Quantitation of guanidine derivatives as representative persistent and mobile organic compounds in water: method development. *Anal. Bioanal. Chem.* 2023, 415, 1953-1965.
32. Brooke, D.N., Nielsen, I.R., Dobson, S., Howe, P.D. Environmental hazard assessment: Di-(2-ethylhexyl) phthalate. TSD 2, 1991. UK Department of the Environment, Garston, United Kingdom.
33. Brix, K.V., Tellis, M.S., Crémazyc, A., Wood, C.M. Characterization of the effects of binary metal mixtures on short-term uptake of Ag, Cu, and Ni by rainbow trout (*Oncorhynchus mykiss*) *Aquatic Toxicol.* 2016, 180, 236–246.
34. Delahaut, V., Chen, P.J., Tan, S.W., Wu, W.L., Rašković, B., Salvado, M.S., Bervoets, L., Blust, R., De Boeck, G. Toxicity and bioaccumulation of Cadmium, Copper and Zinc in a direct comparison at equitoxic concentrations in common carp (*Cyprinus carpio*) juveniles. *PLoS One* 2020, 15, e0220485. doi: 10.1371/journal.pone.0220485.
35. Dubé, M., Auclair, J., Hanana, H., Turcotte, P., Gagnon, C., Gagné, F. Gene expression changes and toxicity of selected rare earth elements in rainbow trout juveniles. *Comp. Biochem. Physiol.* 2019, 223C, 88-95.
36. Chen, P.J., Tan, S.W., Wu, W.L. Stabilization or oxidation of nanoscale zerovalent iron at environmentally relevant exposure changes bioavailability and toxicity in medaka fish. *Environ. Sci. Technol.* 2012, 46, 8431-8239. doi: 10.1021/es3006783.

Disclaimer/Publisher's Note: The statements, opinions and data contained in all publications are solely those of the individual author(s) and contributor(s) and not of MDPI and/or the editor(s). MDPI and/or the editor(s) disclaim responsibility for any injury to people or property resulting from any ideas, methods, instructions or products referred to in the content.